

CONF-850

SLAC-PUB--3864

DE86 007941

SLAC - PUB - 3864
January 1985
(T/E)

RECENT RESULTS FROM DORIS II*

ELLIOTT D. BLOOM

*Stanford Linear Accelerator Center
Stanford University, Stanford, California, 94305*

MASTER

ABSTRACT

This report contains a brief review of recent results from the ARGUS and Crystal Ball experiments at DORIS II, concentrating on T(1S) and T(2S) spectroscopy with a short foray into $\gamma\gamma$ physics.

Presented at the SLAC Summer Institute on Particle Physics,
Stanford, California, July 29 - August 9, 1985.

* Work supported by the Department of Energy, contract DE - AC03 - 76SF00515.

850768--8

(2)

DR-1611-4

30
11/986

1. Introduction

The DORIS II machine has been operating for physics since the end of 1982, with an average luminosity of over $500 \text{ nb}^{-1}/\text{day}$ delivered on a routine basis for the last two years (single days as high as 1600 nb^{-1} have been achieved). The data sample discussed below consists of about 30 pb^{-1} on the 1S, 65 pb^{-1} on the 2S, and 20 pb^{-1} on the 4S and continuum. Figure 1 shows the T system radiative transitions to be discussed in this report. The $\gamma\gamma$ physics discussion will concentrate on two photon final states.

(-)

Cat. 340

2. Radiative Transitions, $T \rightarrow \gamma X$

In the summer of 1984 the Crystal Ball Collaboration first reported evidence for a narrow state at about 1 GeV photon energy, in radiative T(1S) decays corresponding to a mass of 8.3 GeV¹:

$$B[T(1S) \rightarrow \gamma\zeta(8.3)] B[\zeta \rightarrow \text{hadrons}] = (0.47 \pm 0.11 \pm 0.26)\% \quad (1)$$

where the first error is statistical and the second is systematic, depending heavily on the model of the decay for the purported ζ . This result was obtained from 100k T decays.

In the Fall of 1984 more data was taken both at DORIS and CESR, and the 1 GeV photon signal did not reproduce in the new Crystal Ball data² with 200k T decays collected, nor was the state seen by any of the other detectors: ARGUS, CLEO, and CUSB. The values obtained by CUSB³ and CLEO⁴ are respectively,

$$B[T(1S) \rightarrow \gamma\zeta(8.3)] \leq 0.1\% \text{ (90\% C.L.)}, \text{ and, } \leq 0.3\% \text{ (90\% C.L.)} \quad (2)$$

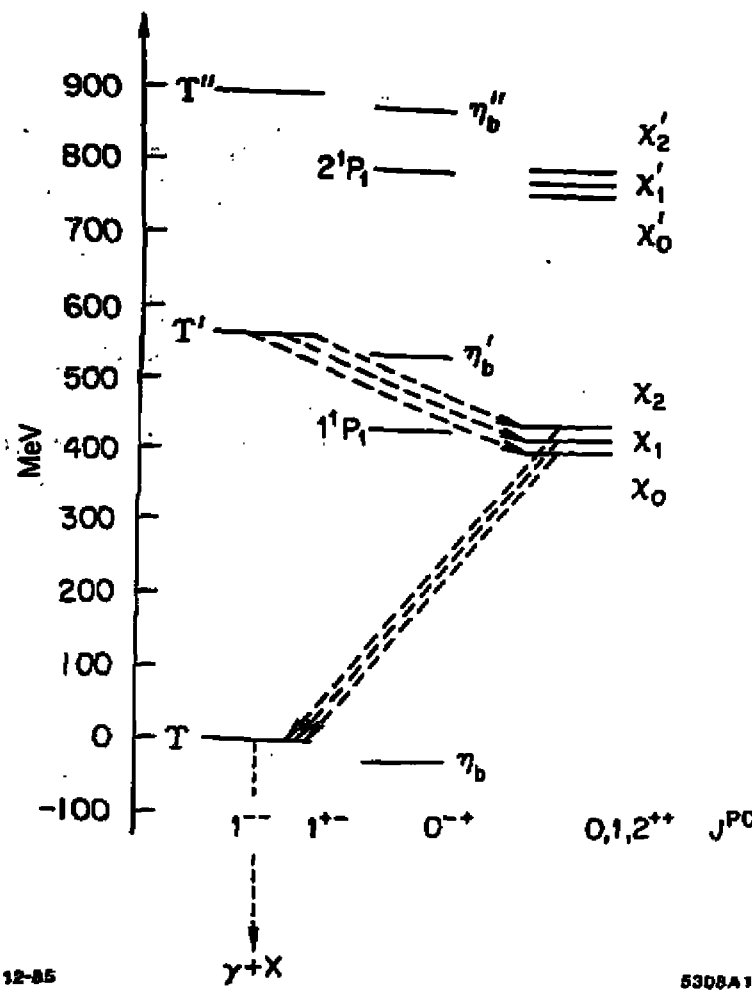


Figure 1: The radiative transitions discussed in this report are shown as dashed lines from the $T(1S)$, $T(2S)$ and the x'_i states.

There is nothing new to report from the Crystal Ball at this time; however, there are new preliminary results to report from the ARGUS detector.

The basic technique used by all experiments was a search for narrow peaks in the inclusive photon spectrum from the $T(1S)$. The detector's photon energy resolution and photon efficiency limits searches of this type along with the statistics of the experiment:

$$90\% \text{ C.L. Limits } \approx 1.3\delta N/[\epsilon \times \#T(1S) \text{ decays}] , \quad (3)$$

where δN is obtained by fitting the inclusive photon spectrum (after cuts have been made) to a "signal" plus polynomial background. A useful approximate relation yielding δN is given by,

$$\delta N \approx \sqrt{N}(1 + (\text{Gaussian Resolution})/(\text{Bin Width})) , \quad (4)$$

where N is the number of counts per bin averaged over the region being fit. The ϵ in Eq. (3) is the efficiency for detecting the photons after all cuts. In the case of the Crystal Ball detector vs. ARGUS: For the CB, $\sigma_E \sim 27$ MeV at 1 GeV, using the NaI(Tl); while for ARGUS, $\sigma_E \sim 10$ MeV at 1 GeV, using converted photons. However, $\epsilon_{CB} \sim 0.2$ (cut and model dependent), while for ARGUS, $\epsilon_{ARGUS} \sim 0.02$ (γ conversion to e^+e^- in thin radiator). Using Eq. (3), we see that the CB and ARGUS should be roughly comparable in sensitivity for observing a narrow state at about 1 GeV photon energy give the same number of Υ decays.

3. ARGUS Preliminary Results on the Search for Narrow Resonances in $T(1S) \rightarrow \gamma X$

Using about 200k $T(1S)$ decays, the ARGUS collaboration has looked in the inclusive photon spectrum in two ways obtaining limits on the branching ratio to narrow states.⁵ The first measurement used converted photons produced in the beam pipe, a thin converter (a few percent of an r.l.), or the inner wall of the drift chamber. The cuts applied were as follows:

- Two tracks of opposite sign produced at a common vertex in the beam pipe, converter, or the inner wall of the drift chamber are required.
- A low χ^2 for the fit is required.
- The angle between the pair of tracks must be less than 18° , and p_T of the charged tracks with respect to the reconstructed direction of the converted photon is less than 0.02 GeV/c.
- The pair mass, $m_{e^+e^-} \leq 0.05$ GeV/c² is required.
- The e^+e^- are identified using DE/DX and/or TOF.
- A π^0 subtraction is made using $E_{\text{conversion}} - E_{\text{shower}}$, where E_{shower} is obtained from the ARGUS Pb-scintillator shower counters.

The resulting efficiency is shown in Fig. 2(a) as the dotted lines. The photon energy resolution obtained is 10 MeV at 1 GeV.

To check the quality of the reconstruction procedure, the invariant mass spectrum of two converted photon was studied by the ARGUS group. Figure 2(b) shows the result of this study. A clear π^0 -signal is observed with a fitted mass for the π^0 of 134.8 ± 0.8 Mev/c², in excellent agreement with the table value.

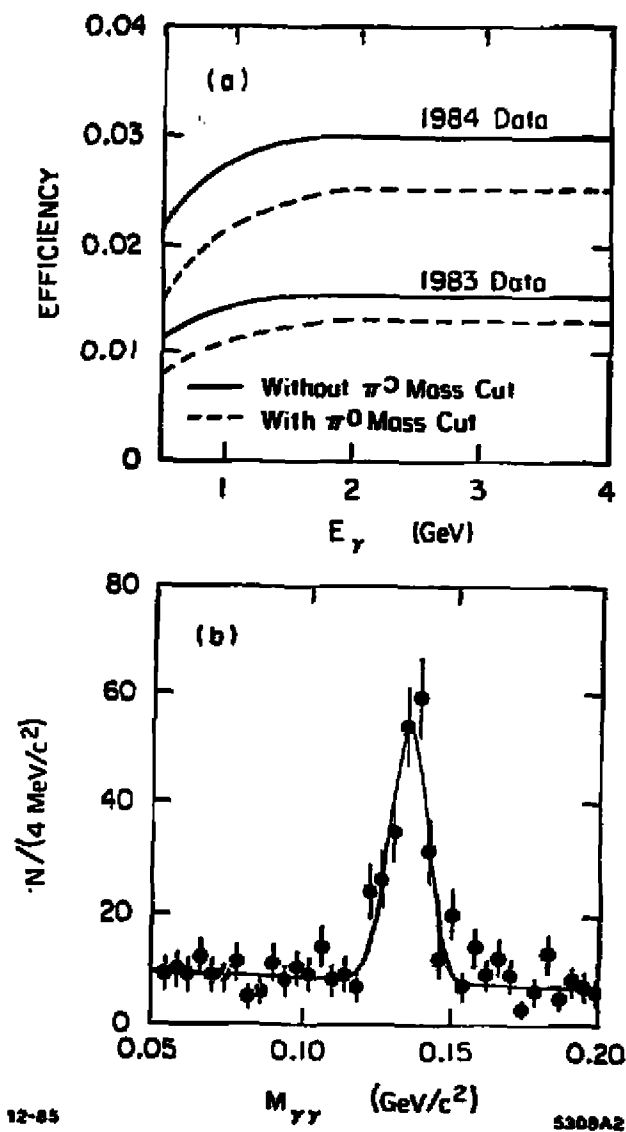


Figure 2: a) The efficiency for detecting conversion photons, in the ARGUS detector, with a π^0 mass cut (dotted lines) and without a π^0 mass cut (solid lines). Curves are shown for the 1983 and 1984 1S data; the 1984 efficiency is somewhat higher since a thicker radiator was used in that run. b) The π^0 mass peak obtained from using multiple converted γ 's per event in the ARGUS detector.

The resulting inclusive photon spectrum from converted photons is shown in Fig. 3(a), and the derived upper limits in Fig. 3(b).⁵ The results shown in this report are preliminary. No significant signal is seen, and the upper limit obtained at the ζ mass for the radiative branching ratio is 0.25% (90% C.L.).

The ARGUS collaboration has also used the Pb - scintillator shower counters to measure the inclusive photon spectrum from $T(1S)$ decays. Only photons detected in the "barrel" shower counters ($|\cos \theta| \leq 0.7$) were used because the background from radiative Bhabha scattering is negligible in this region. This requirement has the further advantage of improving the energy resolution, which is better for the barrel region than for the endcap shower counters ($0.7 \leq |\cos \theta| \leq 0.94$). The resolution for the barrel counters is,

$$\frac{\sigma_E}{E} = \sqrt{(7\%)^2 + (8\%)^2/E} \sim 11\% \text{ at } 1\text{GeV} . \quad (5)$$

Energy clusters resulting from the overlap of charged and neutral particles in neighboring shower counters are identified by the analysis program and removed from further consideration. The main background to the prompt inclusive photon spectrum results from photons from π^0 decay. In the ARGUS analysis this background is suppressed by two cuts, which turn out to be most effective in different energy regions. To reject energy clusters formed by overlapping photons from π^0 decay, transverse cluster shape cuts are used. This cut is most effective in the high energy part of the photon spectrum ($E_\gamma > 0.9$ GeV). To suppress the contribution from low energy π^0 decays, all photons pairs which form a $\gamma\gamma$ mass near the π^0 mass are removed. This cut reduces the background mainly in the low energy part of the photon spectrum ($E_\gamma \leq 1\text{GeV}$). Figure 4(a) shows

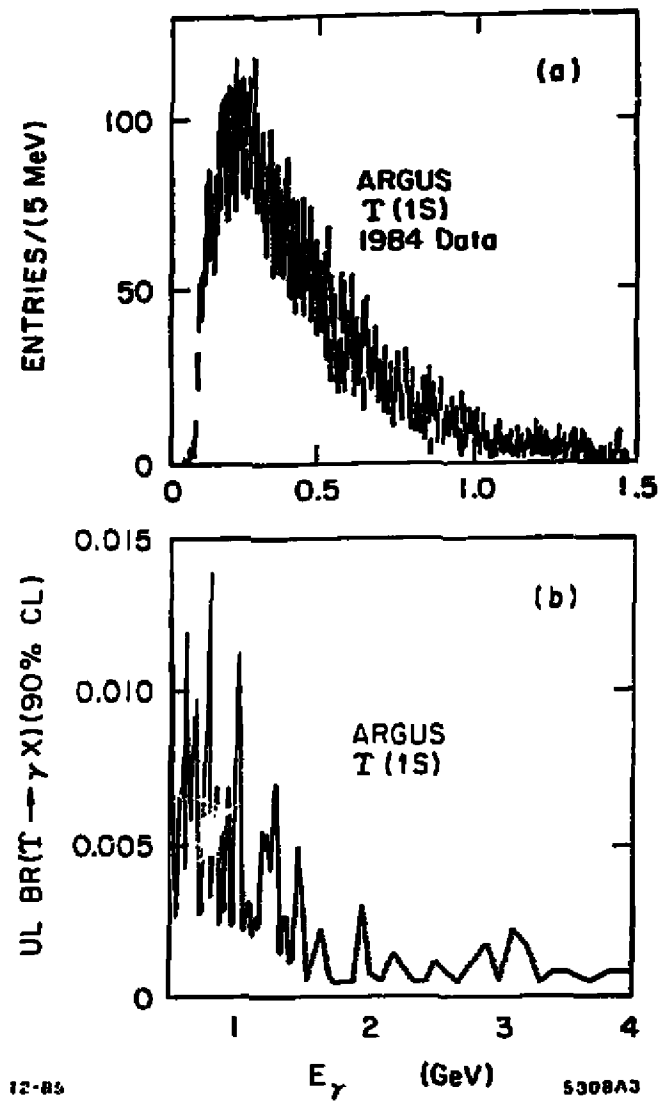


Figure 3: Inclusive photon spectrum from the $T(1S)$ for the ARGUS experiment. Part (a) shows the spectrum observed with the converted photons for the 1984 data and with a π^0 mass cut. Part (b) shows the upper limits obtained from the converted photon data, but by using both 1983 and 1984 data.

the measured photon spectrum after application of the cuts. No significant narrow peak is observed. Figure 4(b) shows the preliminary upper limits obtained by the ARGUS Collaboration from the spectrum of Fig. 4(a). At the ζ mass a preliminary limit of 0.17% (90% C.L.) is obtained on the radiative branching ratio.

In summary, all experiments with results on the inclusive photon spectrum of the T(1S) (ARGUS, CLEO, Crystal Ball, CUSB) have now presented at least preliminary upper limits, and none reproduce the 1984 Crystal Ball evidence for a narrow line at about 1 GeV.

4. Radiative Decays from the T(2S)

The results discussed in this report were obtained by the ARGUS,⁶ CLEO,⁷ Crystal Ball,⁸ and CUSB⁹ experiments. These detectors can be classified as magnetic (ARGUS, CLEO), and NaI(Tl) (Crystal Ball, CUSB). Both magnetic detectors are of the general purpose type employing a magnetic field of about 1 Tesla, good charged particle tracking and momentum resolution using drift chambers, and fair resolution for electromagnetically showering particles using shower calorimeters (see Table 1). A dramatic improvement of the photon energy resolution, at a severe cost in efficiency, can be made by using e^+e^- pairs from converted photons. The conversion may take place either in the beam pipe plus the inner wall of the drift chamber, or in a separate converter placed close to the beam pipe.

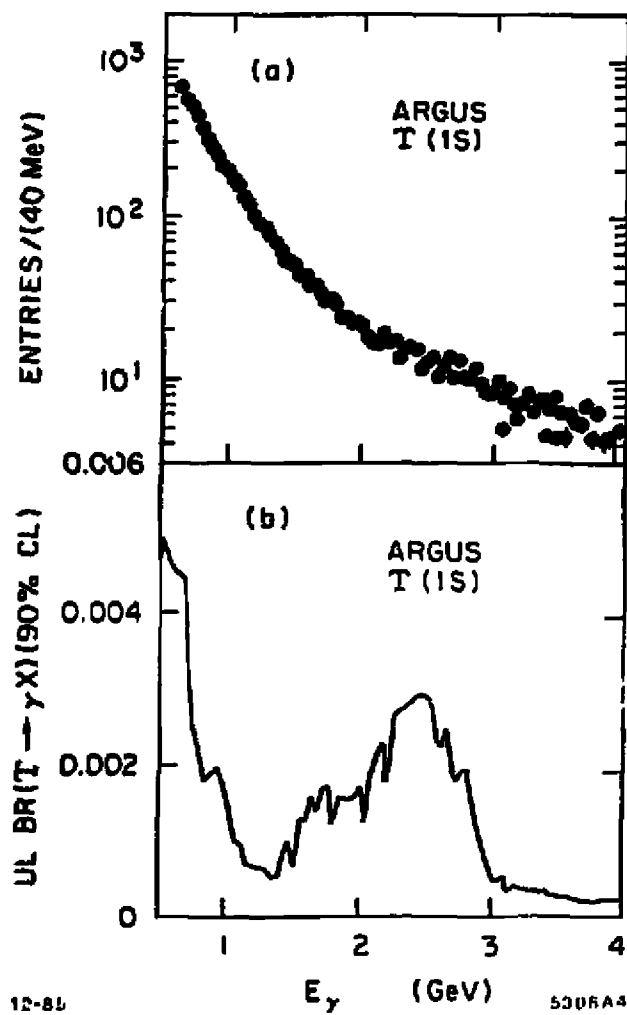


Figure 4: Inclusive photon spectrum from the T(1S) for the ARGUS experiment. Part (a) shows the spectrum observed with the barrel shower counters after a shower shape and a π^0 mass cut. Part (b) shows the upper limits obtained from the barrel shower counter data in part (a).

TABLE 1. Detector parameters relevant to inclusive and exclusive photon measurements for χ_b -state radiation transitions. The σ_p refers to the momentum resolution for charged tracks obtained using drift chambers only. The σ_E is the energy resolution for electromagnetically showering particles in the shower counters. For the detector-specific approaches to inclusive analyses (see text), typical resolution (σ_{γ}) and efficiency (ϵ_{γ}) values at 100 MeV are shown.

	ARGUS	CLEO	CRYSTAL BALL	CUSB
Magnetic Field	0.8T	1.0T	-	-
$\sigma_p/p(\text{GeV}/c)(\%)$	$\sim 1.2 \times p$	$\sim 1.2 \times p$	-	-
$\sigma_E/E(\text{GeV})(\%)$	$(7^2 + 5^2/E)^{1/2}$	$17/E^{1/2}$	$2.7/E^{1/4}$	$4/E^{1/4}$
σ_{γ} , at 100 MeV	1.1 MeV	2.5 MeV	4.8 MeV	7.1 MeV
ϵ_{γ} , at 100 MeV	0.2%	2%	15%	13%

The NaI(Tl) detectors are optimised for the detection of low energy photons. However, with presently operating detectors, the best photon resolution is obtained by the magnetic detectors, via photon conversion, in the low energy range of the χ_b -state transitions.

Figure 5 shows the energy dependence of the photon energy resolution (part (a)), and efficiency (part (b)) in a multihadronic final state environment. The superior energy resolution of the magnetic detectors over this energy range is apparent. This is to be contrasted with the very low and rapidly varying photon detection efficiency for the magnetic detectors. The NaI(Tl) detectors have a relatively large efficiency which only has a weak dependence on the photon energy. Therefore, one might expect complementary results from these two classes of detectors: more accurate branching ratios, and cascade measurements from the NaI(Tl) detectors, and better measurement of the χ_b -state masses from the

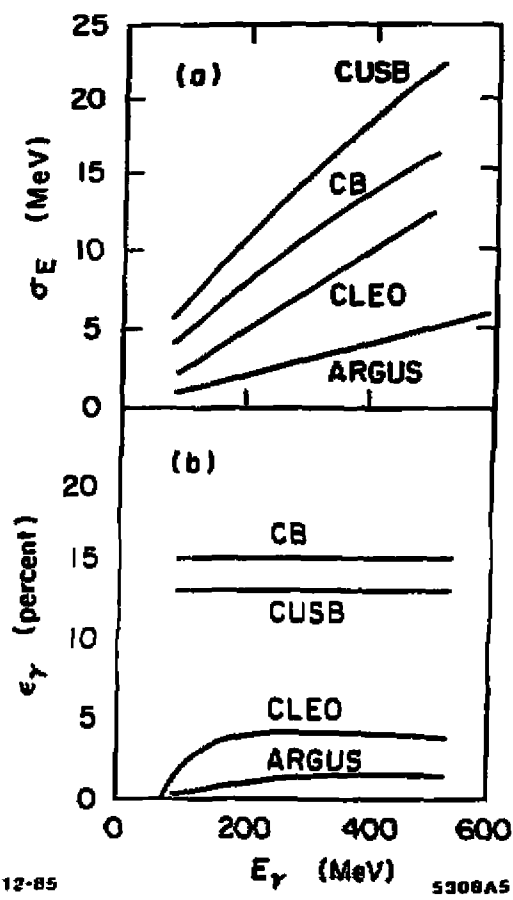


Figure 5: Approximate photon energy resolution functions, part (a), and efficiencies, part (b), for photon energies in the range of the χ_b -state transition energies for the four detectors discussed in the text. The non-magnetic CUSB and Crystal Ball detectors use NaI(Tl) to measure the photons, while the magnetic detectors measure the e^+e^- pairs from converted photons.

magnetic detectors. How well each pole is realized will depend on the separation of the χ_5 -states achieved, the statistical significance of the observed lines, as well as other details.

All four experiments have obtained results on the radiative transitions $T(25) \rightarrow \gamma \chi_5'$. The transitions can be studied in two ways, either by observing the inclusive photon spectrum, or by analyzing the fully exclusive cascade decay. In the latter case, the χ_5' state is required to decay radiatively to the $T(15)$, which in turn is required to decay into two muons or two electrons. As mentioned above, only the NaI(Tl) detectors are able to study the exclusive cascade reaction.

The first results on the χ_5' states were reported by the CUSB detector,⁶ and later by CLEO.⁷ (Note that CLEO has reanalyzed their data and their latest results are presented in this report.) Figures 6(a) and 6(c) shows the results on the inclusive photon spectrum from these two detectors. Both experiments agree well on the position of the two lowest energies at about 108 and 128 MeV; however, the third line is only poorly measured at best. CUSB unfolded the energy of the line from their spectrum at an energy of about 149 MeV. CLEO had an indication for a line at about 165 MeV, but with less than two standard deviation significance. If the "bump" in the CLEO spectrum at about 149 MeV is forced to coincide in energy and branching ratio with the CUSB values, consistency with the data is obtained within error. Thus more measurements were needed to settle the question of the third line.

The Crystal Ball had the necessary energy resolution and by the summer of 1984 had accumulated enough statistics to make a significant measurement of the third line.⁸ Impressive results from ARGUS⁹ soon followed which confirmed the Crystal Ball results, and provide the best measurement of the energy of the

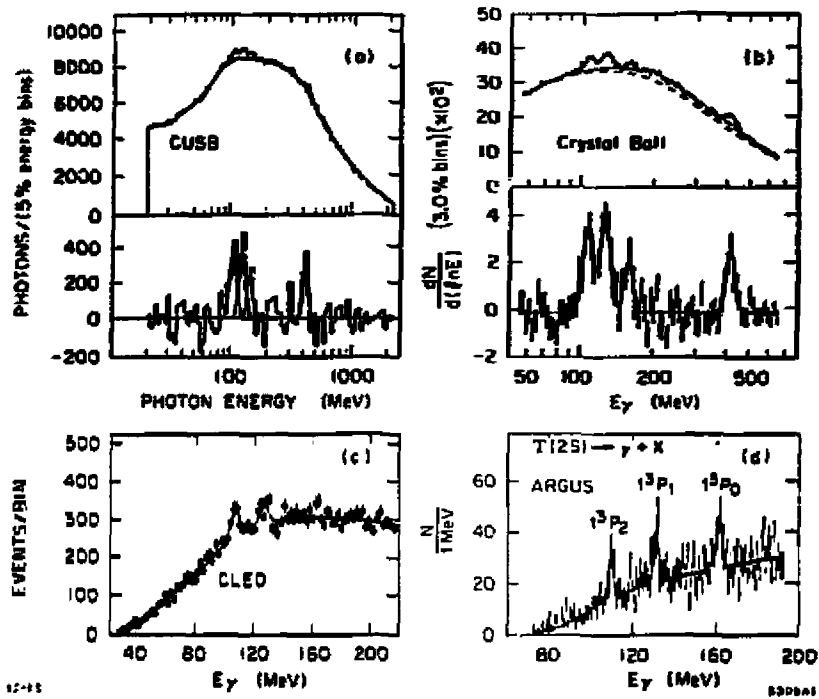


Figure 6: The $T(2S)$ inclusive photon spectra from the experiments discussed in the text and in the order of improving photon resolution. a) Results from the CUSB experiment; the background subtracted spectrum is shown below the full spectrum. b) Results from the Crystal Ball experiment; the background subtracted spectrum is shown below the full spectrum. c) Results from the CLEO experiment using converted photons. The bump at 149 MeV in the fit is forced to coincide in energy and branching ratio with the corresponding CUSB measurement. The fit prefers a photon energy of about 165 MeV. d) Results from the ARGUS experiment using converted photons. Note the very good energy resolution in this energy range of about $\sigma_E \sim 1.1$ MeV.

lines. Figures 6(b) and 6(d) show these spectra. The two measurements from DORIS II confirm the original CESR measurements on the two lowest energy lines. The highest energy third line is firmly established at about 162 MeV.

Table 2 collects the results on the photon energies and branching ratios, while a plot of these measurements is given in Fig. 7. The energies obtained in inclusive and exclusive (see the next section) reactions by the NaI(Tl) detectors have been averaged using weighted means. Statistical and systematic errors have also been combined in quadrature to allow an easier comparison. The last row of Table 2 shows the average of all measurements. The CLEO value on the third line are omitted from the averages as this line was claimed as not significant in their data. Although the CUSB highest energy line disagrees with the other experiments, the average energy and branching ratio change very little (within the errors) when the CUSB values are excluded. This is due to the relatively precise measurements of ARGUS, and the similarity in all branching ratios for the third line.

Although all experiments agree on the energies of the two lowest transitions, the branching ratio results from the magnetic detectors appear systematically higher than those from the NaI(Tl) detectors, though the errors are large. This may be due to a systematic difference in the results from the two types of detectors, for as described above, a small and rapidly varying photon efficiency is a characteristic of the magnetic detectors in this photon energy range relative to the NaI(Tl) detectors.

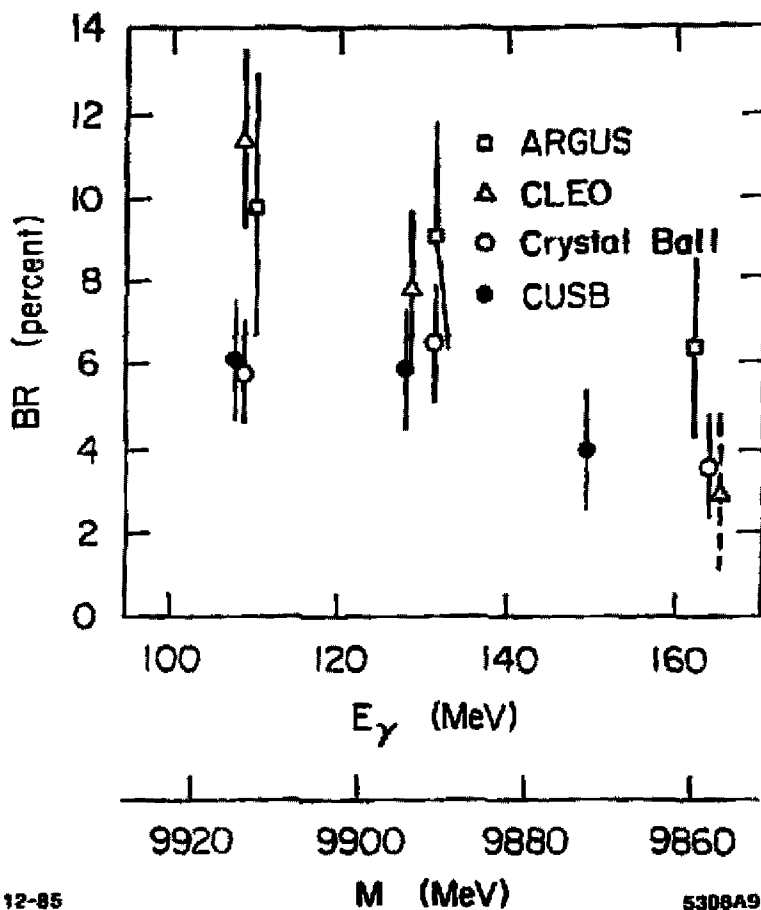


Figure 7: The measurements of $T(2S) \rightarrow \gamma \chi_1^0$: E_γ and branching ratios from the four experiments are shown and discussed in the text. Plotted is the branching ratio versus the photon energy. For the NaI(Tl) experiments, inclusive and exclusive measurements from the same experiment have been averaged using weighted means. Systematic errors are added in quadrature.

TABLE 2. Photon energies and branching ratios measured by the four experiments discussed in the text. Note that the results on the photon energies from the NaI(Tl) detectors are an average of their inclusive and exclusive results. Weighted means are used to calculate the overall world averages. The measurements by CLEO on the highest energy line are not included in the average, as their data do not unambiguously imply this state.

Experiment	Photon Energy (MeV)	Branching Ratio (%)
ARGUS	110.6 ± 0.9	9.8 ± 3.2
	131.7 ± 1.1	9.1 ± 2.8
	162.1 ± 1.5	6.4 ± 2.1
CLEO	109.0 ± 0.7	11.4 ± 2.1
	128.6 ± 1.0	7.8 ± 1.9
	(165.1 ± 2.8)	(3.0 ± 1.8)
CRYSTAL BALL	108.2 ± 1.6	5.8 ± 1.2
	131.4 ± 1.5	6.5 ± 1.4
	163.8 ± 3.1	3.6 ± 1.2
CUSB	107.7 ± 1.5	6.1 ± 1.4
	128.0 ± 1.3	5.9 ± 1.4
	149.4 ± 5.0	3.5 ± 1.4
Average	109.3 ± 0.5	7.0 ± 0.8
	130.0 ± 0.6	6.8 ± 0.8
	161.6 ± 1.3	4.0 ± 0.8

5. The Cascade Reaction and the Spin of the χ_b -states

Results on the cascade reaction, $T(2S) \rightarrow \gamma \chi_b^J \rightarrow \gamma \gamma T(1S) \rightarrow \gamma \gamma e^+ e^-$ and $\mu^+ \mu^-$, were first obtained by the CUSB¹⁰ experiment. These results have been confirmed by the Crystal Ball.¹¹ Figure 8 shows the results from both experiments. Only the two lowest lying photon transitions are seen in this reaction. Only upper limits are available for the third line. The value obtained from the Crystal Ball experiment for the cascade branching ratios are,

$$\begin{aligned} BR[T(2S) \rightarrow \gamma \chi_b^\alpha] \times BR[\chi_b^\alpha \rightarrow \gamma T] &= (1.6 \pm 0.3 \pm 0.3)\% , \\ BR[T(2S) \rightarrow \gamma \chi_b^\beta] \times BR[\chi_b^\beta \rightarrow \gamma T] &= (2.1 \pm 0.3 \pm 0.4)\% , \end{aligned} \quad (6)$$

and

$$BR[T(2S) \rightarrow \gamma \chi_b^\gamma] \times BR[\chi_b^\gamma \rightarrow \gamma T] < 0.2\% \text{ (90\% C.L.)} ,$$

where, α , β and γ indicate the lowest to highest energy first photon transitions. Combining the above numbers with the Crystal Ball inclusive photon branching ratios yield,

$$\begin{aligned} BR(\chi_b^\alpha \rightarrow \gamma T(1S)) &= (27 \pm 6 \pm 6)\% , \\ BR(\chi_b^\beta \rightarrow \gamma T(1S)) &= (32 \pm 6 \pm 7)\% , \end{aligned} \quad (7)$$

and

$$BR(\chi_b^\gamma \rightarrow \gamma T(1S)) \leq 6\% \text{ (90\% C.L.)} .$$

The angular correlations of the photons emitted in the cascade decay depend on the spins of the χ_b^J states. Though the statistics are limited, the good separation of the two states and the low background in the Crystal Ball results allows a convincing, though model dependent, determination of the spin of the χ_b states to be carried out.¹²

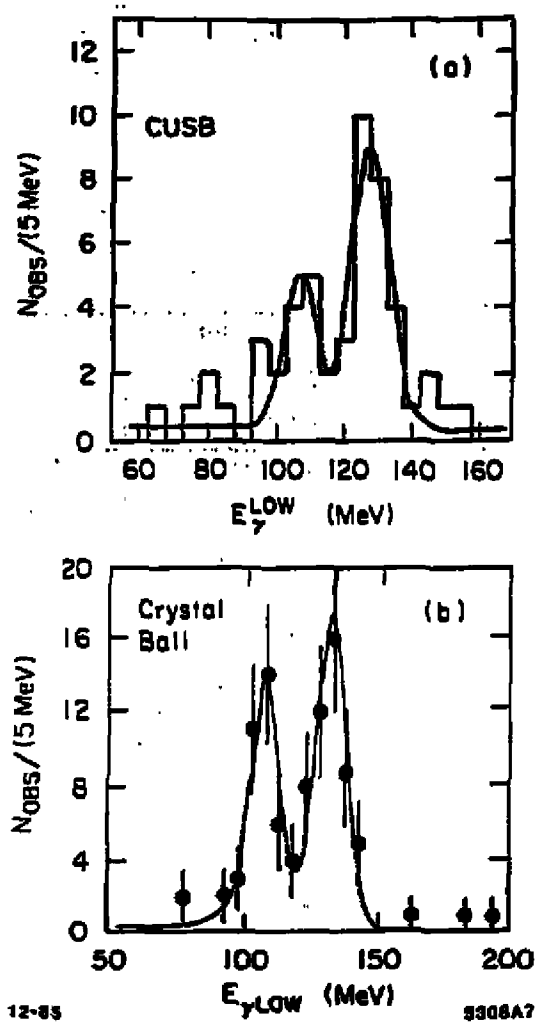


Figure 8: The $T(2S)$ exclusive cascade spectra from the a) CUSB experiment, and b) Crystal Ball experiment. The lower of the two photon energies is plotted vs. number of events per 5 MeV.

Given the limited statistics, an attempt is made to extract the maximum information about the χ_b spins by analysing the full angular correlation in the cascade reaction. The full angular distribution is described by six independent angles (the directions of the two photons and the directions of the two leptons - back to back in the $T(1S)$ rest frame). The angular distributions also depend on the χ_b spin (J), the relative strength of the transition multipoles, and the e^+e^- beam polarization (measured at the $T(2S)$, by the Crystal Ball experiment using the angular distribution in $e^+e^- \rightarrow \mu^+\mu^-$, to be $P = 75 \pm 5\%$).

The analysis was model dependent in a few ways. First, in accordance with the quarkonium model, only $J = 0, 1, 2$ for the χ_b^J states were considered. Second, relying on non-relativistic approximations, the transition matrix elements were assumed to be electric dipole for both cascade transitions. Crystal Ball results on the charmonium system,¹³ indicate dipole dominance within large errors. The bottomonium system, being less relativistic than charmonium, is expected to have the higher multipoles suppressed by an order of magnitude¹⁴ as compared to charmonium.

After the transition multipoles and the beam polarization value are fixed, the angular distribution in the cascade transitions depends only on the χ_b^J spin. The theoretical formulae for these distributions can be found in Ref. 14.

In the standard bottomonium model, $J_\alpha = 2$ and $J_\beta = 1$ (for $\chi_b^\alpha, \chi_b^\beta$). One expects that the relatively rapid varying angular distribution for $J = 0$ as compared to $J = 1, 2$ will allow exclusion of $J = 0$ for these states. The first step of the Crystal Ball analysis is thus to use the logarithmic likelihood for $J = 0$,

$$\frac{1}{N} \sum_{i=1}^N \ln W_{J=0}(\Omega_i) , \quad (8)$$

as a test function for testing the different spin hypotheses. In Eq. (8) the Ω_i denotes the measured values of all six independent angles in the i^{th} event, N is the number of events in the data sample and $W_J(\Omega_i)$ is the theoretical formula for the angular correlation function for spin J .

To obtain the theoretical distributions, Monte Carlo (M.C.) events were generated according to each spin hypothesis. The generated events were passed through a simulation of the detector, and the same cuts were then applied as to real events. Typically 70k M.C. events were processed for each case of a given test function and spin assumption, and a mean and σ for the assumed Gaussian likelihood function were estimated. In one case 10^6 events were generated and the surviving M.C. events were grouped into a large number of experiments with the same statistics as found in the true data sample. The likelihood functions obtained in these cases were Gaussian to the few σ level (limited by statistics). Due to the limits of computer time the full detector simulation was not used for the 10^6 event test case.

The experimental data sample was obtained by essentially splitting the two observed peaks down the middle. There is a small background of about 12% for the χ_b^α and 6% for the χ_b^β states coming mainly from the finite energy resolution of the NaI(Tl). The data are evaluated for the same test function as the M.C. events yielding one value per test function. Figures 9(a) and 9(b) show the result for the test function for spin 0 on the χ_b^α and χ_b^β data samples respectively. The curves are the (assumed Gaussian) distributions for the various labeled M.C. The J values evaluated are under the $J = 0$ test function. Spin 0 is excluded for the two states with C.L. > 99.5%.

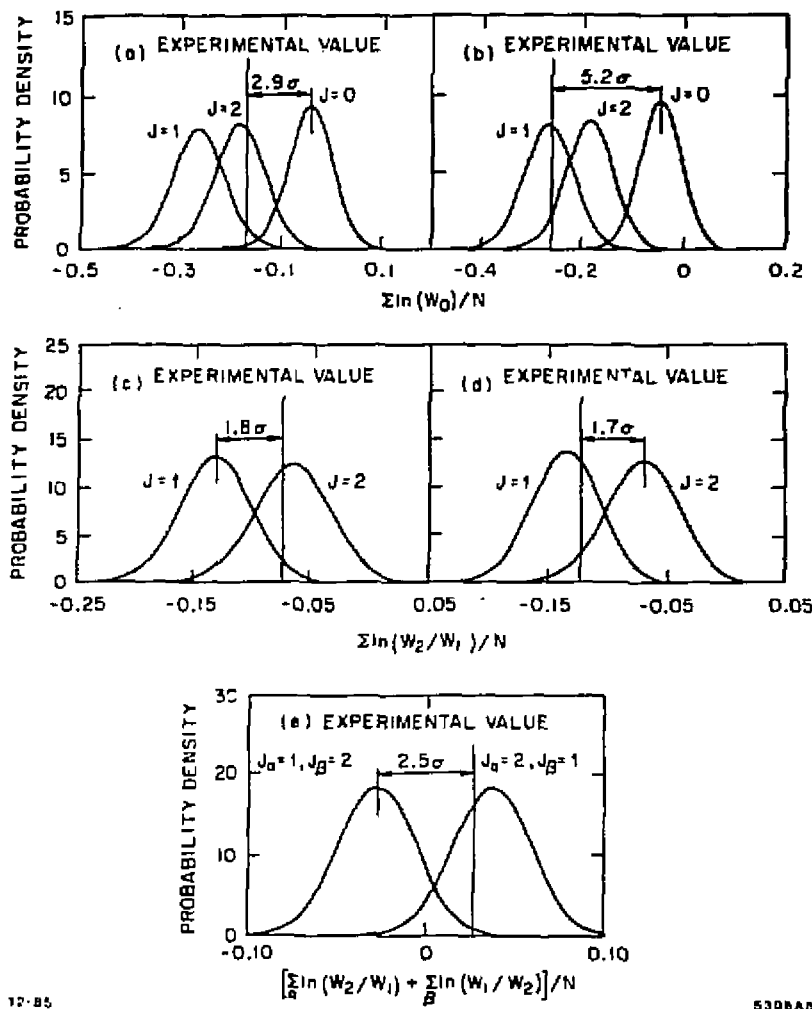


Figure 9: Likelihood tests for the spin of the χ_b^J states using the $\gamma\gamma l^+l^-$ cascade $\Upsilon(2S)$ events from the Crystal Ball. The single experimental value is compared through the indicated test functions (see text). The χ_b^α state results from the lower energy first photon, the χ_b^β state the higher energy photon. a) Tests for spin 0 of the χ_b^α sample; predicted spin is $J=2$. b) Tests for spin 0 of the χ_b^β sample; predicted spin is $J=1$. c) Likelihood ratio tests for the χ_b^α sample; predicted spin is $J=2$. d) Likelihood ratio tests for the χ_b^β sample; predicted spin is $J=1$. e) Likelihood ratio tests for the combined data of the χ_b^α and χ_b^β samples; predicted spins are $J_\alpha = 2, J_\beta = 1$.

One may apply other test functions to distinguish between $J = 1$ and 2 . A standard test function¹⁵ is given by,

$$\frac{1}{N} \sum_{i=1}^N \ln [W_{J=2}(\Omega_i) / W_{J=1}(\Omega_i)] . \quad (9)$$

Figures 9(b) and 9(c) show the result for this test function on the x_b^a and x_b^s data samples. The data favor the spins expected in the quark model; however, this test does not strictly rule out the reverse spin assignments.

A decisive test can be made under the assumption that only $J=1$ and 2 are the remaining possibilities to be assigned to x_b^a and x_b^s . In this case the test function used is,

$$\frac{1}{N_a + N_s} \left\{ \sum_{i=1}^{N_a} \ln [W_{J=2}(\Omega_i) / W_{J=1}(\Omega_i)] + \sum_{i=1}^{N_s} \ln [W_{J=1}(\Omega_i) / W_{J=2}(\Omega_i)] \right\} . \quad (10)$$

Figure 9(e) shows the results of the comparison of the data with this compound test function. The wrong spin combination is ruled out at C.L. > 98%. Thus the values expected in the quark model of $J_a = 2$ and $J_s = 1$ are obtained.

Additional information concerning the spins of the x_b^J states comes from the inclusive radiative transition rates. Under the assumptions of the applicability of the non-relativistic quark model and dipole dominance for the transitions from the $T(2S)$ to the x_b^J states, the relative "strengths" of these transitions are proportional to $E_\gamma^J (2J + 1)$. If relativistic and mixing effects are neglected, the

matrix elements for the transitions should be the same for all three x_b^J states,

$$\Gamma(S \rightarrow P) = \frac{4}{9} \frac{(2J_f + 1)}{(2J_i + 1)} Q^2 \alpha |E_{if}|^2 E_\gamma^3 , \quad (11)$$

and $E_{if} = \int_0^\infty dr r^3 [\psi_i(r) \psi_f(r)]$.

Using the rates measured by the Crystal Ball the results of Table 3 are obtained. Not all cases are shown in the table and those shown are representative. This test, which has somewhat different operative assumptions than the cascade angular distribution test, also strongly favors the quarkonium model predictions for the x_b^J state spins, i.e., $J_\alpha = 2$, $J_\beta = 1$ and $J_\gamma = 0$.

TABLE 3. The ratio of inclusive photon branching ratios of the Crystal Ball to $(2J_f + 1) \times E_\gamma^3$, relative to the 1^3P_1 , ratio. This ratio of ratios is examined vs. the assumed J order for the x_b^α , x_b^β , and x_b^γ states, where x_b^α is associated with the lowest energy first photon transition, x_b^γ the highest. The expected quarkonium J order of 2, 1, 0 yields ratios consistent with 1 within error; 1 is the value expected in the non-relativistic quarkonium model. Other J orders yield ratios not consistent with 1. The values shown in the table are representative of all J orders, with only J order 2, 1, 0 yielding ratios consistent with 1.

J Order $x_b^\alpha, x_b^\beta, x_b^\gamma$	$\left\{ \frac{BR(3^3S_1 \rightarrow 1^3P_f)}{(2J_f + 1) \times E_\gamma^3} \right\}$ divided by $\left\{ \frac{BR(3^3S_1 \rightarrow 1^3P_1)}{3 \times E_\gamma^3} \right\}$
2, 1, 0	$0.89 \pm 0.27 : 1 : 0.84 \pm 0.33$
1, 2, 0	$2.46 \pm 0.74 : 1 : 1.40 \pm 0.55$
0, 1, 2	$4.92 \pm 1.21 : 1 : 0.15 \pm 0.06$

6. Meson Formation by Photon-Photon Collisions

The Crystal Ball has looked for meson formation in photon-photon collisions¹⁶ where the meson decays into two or four γ 's. The events are not tagged; the cuts used to establish the $\gamma\gamma$ origin of the events are as follows:

- all neutral final state
- $E_{\text{seen}} \leq E_{\text{cm}}$
- approximate p_{\perp} - balance in the event.

The possible final states for four photons are $\pi^0\pi^0$, $\pi^0\eta$, $\eta\eta$, Examination of 110 pb^{-1} of data has resulted in measurements of the properties of A_2 and $\delta(980)$ formation,¹⁷ which have recently been published.

The Crystal Ball has also investigated the two-photon final state to determine the $\gamma\gamma$ coupling of pseudoscalar mesons. In a run with special trigger conditions, 6.8 pb^{-1} were taken to investigate the reaction $\gamma\gamma \rightarrow \pi^0 \rightarrow \gamma\gamma$. As the energy seen in the detector is very low, background from beam-gas reactions is important and has been measured in runs with separated beams. The $\gamma\gamma$ mass spectrum is shown in Fig. 10(a) before beam-gas subtraction. Signals at the π^0 , η , and η' masses are seen (the η and η' are marginal in this data using the special trigger, but have been clearly seen when adding in all available data). Figure 10(b) shows the region of the π^0 peak after beam-gas subtraction. A fit yields 124 ± 22 π^0 events; the resulting mass and sigma of the π^0 peak are $134.5 \pm 1.0 \text{ MeV}$, and $5.1 \pm 0.9 \text{ MeV}$ respectively. This yields a total width $\Gamma_{\pi^0} = (7.9 \pm 1.4 \pm 1.6) \text{ ev}$ (preliminary).¹⁸ At the time of this conference, more data with the π^0 trigger are being taken, there is however no hope to surpass the accuracy of the result of Ref. 18. The purpose of this investigation is to

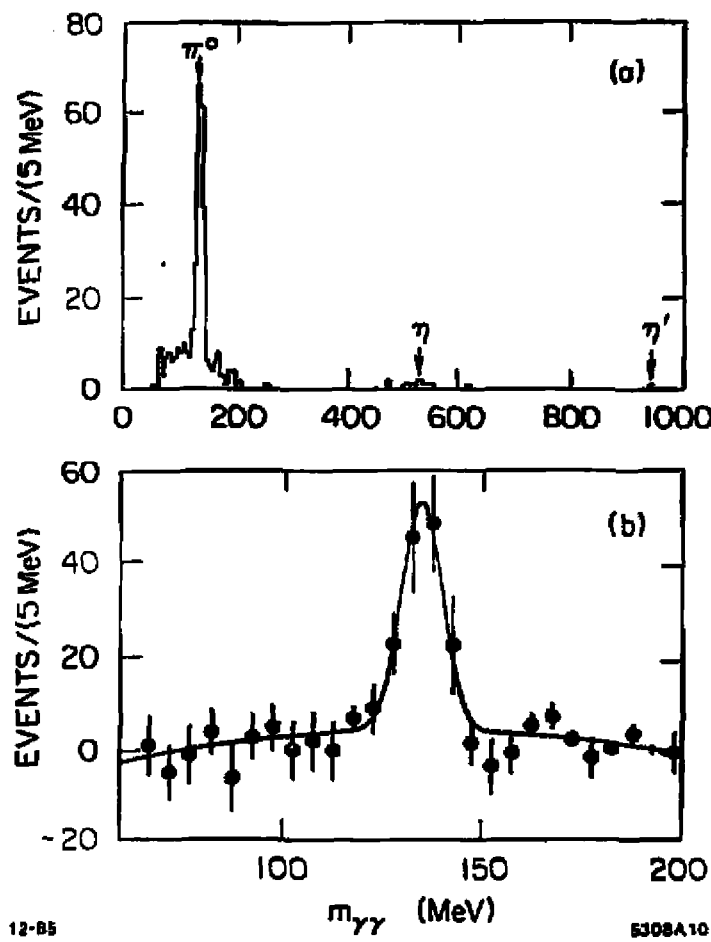


Figure 10: Two-photon final state from photon-photon collisions using the Crystal Ball detector. a) The $\gamma\gamma$ mass spectrum from the π^0 to the η' . b) The region of the π^0 after background subtraction using separated beam data and showing the fit to the data used to extract the number of π^0 's.

cross-check the method of $\gamma\gamma$ scattering for e^+e^- storage rings in general and the analysis of all-photon final states in the Crystal Ball experiment in particular.

7. Conclusions

- The existence of the $\zeta(3.2)$ is very unlikely given the recent preliminary results of the ARGUS, Crystal Ball, and CUSB experiments (CLEO results are less restrictive).
- The energies and transition rates for the x_1^0 states have been well measured. There are three states.
- The spins of the x_1^0 states are as expected in quarkonium models.
- Two-photon interactions continue to be a productive source of information for mesons with mass less than 2 GeV.

ACKNOWLEDGEMENTS

I would like to thank the many members of the Crystal Ball and ARGUS Collaborations who contributed to this report. In some cases extensive conversations were held before I got things right. In particular, I would like to thank J. Prentice, K. Königsmann, S. Lowe, T. Skwarnicki, and K. Wacker. I have heavily relied on their work in producing this report.

REFERENCES

1. Crystal Ball Collaboration, Peck, C., SLAC-PUB-3380 and DESY 84-084, (1984); Trost, H., *Proceedings of the XXII International Conference on High Energy Physics*, Leipzig, DDR, July 19-25, 1984; Niczyporuk, B., *Proceedings of the SLAC Summer Institute on Particle Physics*, Stanford University, Stanford, CA, July 23-August 3, 1984; Coyne, D.G., *Proceeding of the Conference on Physics in Collision IV*, University of California at Santa Cruz, Santa Cruz, California, August 22-24, 1984.
2. E.D. Bloom, Crystal Ball Collaboration, SLAC-PUB-3686 and *Proceedings of the 5th Topical Workshop on Proton Antiproton Collider Physics*, St. Vincent, Italy, February 25-March 1, 1985;
S.T. Lowe, Crystal Ball Collaboration, SLAC-PUB-3683 and *Proceedings of the XXth Rencontre de Moriond*, Les Arcs, France, March 10-17, 1985.
3. J. Lee-Franzini, CUSB Collaboration, *Proceeding of the 5th International Conference on Physics in Collision*, Autun, France, July 3-5, 1985.
4. D. Peterson, CLEO Collaboration, *Proceedings of the International Conference on Hadron Spectroscopy*, College Park, Maryland, April 20-22, 1985.
5. H. Albrecht *et al.*, DESY 85-083 (1985), submitted to *Zeit.Phys.*
6. H. Albrecht *et al.*, *Phys. Lett.* 160B,331 (1985).
7. P. Hamm *et al.*, *Phys. Rev. Lett.* 52,799 (1984).
8. R. Nernst *et al.*, *Phys. Rev. Lett.* 54,2195 (1985).
9. C. Klopfenstein *et al.*, *Phys. Rev. Lett.* 51,160 (1983).
10. F. Pauss *et al.*, *Phys. Lett.* 130B,439 (1983).

11. W. Walk et al., SLAC-PUB-3575 and DESY 85-019, submitted to Phys. Rev. D (1986).
12. T. Skwarnicki, Crystal Ball Collaboration, DESY 85-042 (1985) and *Proceedings of the 22nd Rencontre de Moriond*, Les Arcs, France, March 10-17, 1985.
13. M. Oreglia et al., Phys. Rev. D 25, 2259 (1982).
14. L. S. Brown, R. N. Cahn, Phys. Rev. D 13, 1195 (1976).
15. See for instance: W. T. Eadie et al., Statistical Methods In Experimental Physics, North-Holland, Amsterdam (1971), p.224.
16. K. Wacker, *Proceedings of the International Conference on High Energy Physics*, Bari, Italy, July 18-24, 1985; D. Williams, *Proceedings of the 6th Int. Workshop on Photon-Photon Collisions*, Lake Tahoe, Calif., U.S.A., (1984).
17. D. Antreasyan, et al., SLAC-PUB-3761 and DESY 85-97, to be published in Phys. Rev. D (1986).
18. H. W. Atherton, et al., Phys. Lett. 158B, 81 (1985).